ACS Catalysis

Research Article

pubs.acs.org/acscatalysis

Creation of Nickel-Based Active Species within a Macroreticular Acidic Resin: A Noble-Metal-Free Heterogeneous Catalyst for Visible-Light-Driven H_2 Evolution from Water

Kohsuke Mori,*[,†,‡] Hiroki Kakudo,[†] and Hiromi Yamashita*[,†,‡]

[†]Division of Materials and Manufacturing Science, Graduate School of Engineering, Osaka University, 2-1 Yamada-oka, Suita, Osaka 565-0871, Japan

[‡]ESICB, Kyoto University, Katsura, Kyoto, Kyoto 615-8520, Japan

Supporting Information

ABSTRACT: An acidic resin bearing $-SO_3^-$ functional groups within its macroreticular structure acts as an efficient support for *in situ* formation of a noble-metal-free Ni-based catalyst responsible for visible-light-driven H_2 production from water. Characterization by means of XAFS revealed that simple ion-exchange of the resin with a trinuclear Ni complex, $Ni(NiL_2)_2Cl_2$ (L = β-mercaptoethylamine), affords monomeric Ni(II) species involving β-mercaptoethylamine and aqua ligands in an octahedral coordination geometry, which is easily transformed into real active species containing a TEOA ligand during the initial induction period of the photocatalytic reaction. Such *in situ*-generated Ni species offer a simple and efficient photocatalytic system whose activity is five times greater than that of its homogeneous counterpart, enabling efficient H_2 production when xanthene dye is employed as a visible-light-responsive photosensitizer. The acidity of the resins as well as β-mercaptoethylamine and the TEOA ligands were found to be key factors in achieving efficient catalytic performance. Moreover, leaching and agglomeration of the active Ni species were not observed, and the recovered catalyst could be recycled without significant loss of activity.

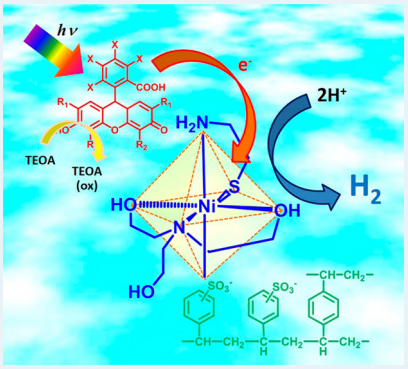

KEYWORDS: *acidic resin, Ni complex, H_2 production, photocatalysis, visible-light, noble-metal-free*

INTRODUCTION

Efficient conversion of solar energy into stored chemical potential via environmentally friendly artificial photosynthesis is a promising approach to providing carbon-free energy for sustainable development.[1,2] Because of this potential, photochemical H_2 generation driven by visible-light irradiation in an aqueous medium has been the subject of much interest.[3−5] A variety of heterogeneous systems based on semiconducting metal oxides have been examined for water splitting into H_2 and O_2 since the late 1970s,[6] and considerable successes have been attained based on band gap engineering.[7−10]

Molecular-based photosystems have also been extensively studied from the point of view of photoinduced H_2 production.[11−14] Transition metal complexes have a distinct advantage because their photophysical properties can be tuned by precise ligand modification.[15] Molecular-based photocatalytic H_2 production systems commonly involve multiple components, including a photosensitizer (PS) responsible for the absorption of visible light, in conjunction with an electron relay (ER), a water reduction catalyst (WRC) to produce H_2, and sacrificial reagents (SR) to provide the electron replenishing of the PS unit. The overall reaction is considered to be a visible-light-driven proton reduction process by SR to form molecular H_2 via electron relay. Traditionally, $[Ru(bpy)_3]^{2+}$ (bpy = 2,2′-bipyridine) has been utilized as a PS and platinum is well established as a WRC metal.[16] However, frequent use of the precious metal Pt has sparked widespread interest in the possibility of using abundant and inexpensive metal complexes for WRC. Several promising examples of photocatalytic hydrogen evolution using catalysts consisting of Fe, Co, and Ni complexes sensitized by nonprecious-metal-containing PSs are found in the literature.[17−21] Unfortunately, the use of such metal complexes faces practical problems due to the necessity of using large amounts of organic solvents and difficulties in recovering the expensive transition metals and ligands.

Ion-exchange resins have been extensively employed in various separation, purification, and decontamination processes.[22] Although the thermal stability is relatively low compared to inorganic supports, such as zeolites and mesoporous silicas,[23] the unique characteristics of functional resins, including relatively high surface areas originating from their porous structure, acidic/basic and hydrophilic/hydrophobic properties, ease of introduction of a wide variety of functional groups, and their ability to swell in reaction media, make these materials very attractive from the viewpoint of

Received: August 1, 2014
Revised: October 10, 2014
Published: October 14, 2014

   dx.doi.org/10.1021/cs501119d | ACS Catal. 2014, 4, 4129−4135

catalyst design.[24] Additionally, these resins can be utilized to stabilize metal complexes and metal nanoparticles (NPs) inside macroreticular domains with controllable morphology and practical thermal and mechanical stability, offering promising catalyst support for a number of industrial processes.[25−27] It is well accepted that the existence of suitable surface functional groups in the vicinity of active metal centers exerts a beneficial impact on catalytic performance.[28] Furthermore, swelling properties can result in dramatic improvements in the accessibility of reactants in the liquid phase. Consequently, the use of functional resin matrices provides unexceptional catalytic functions that cannot be attained by homogeneous counterparts, such as site isolation of well-defined active species and cooperative action by several sites.

In this paper, we present a new catalyst created by simple ion exchange of a trinuclear complex, $Ni(NiL_2)_2Cl_2$ (L = β-mercaptoethylamine) with a cation-exchange resin possessing strongly acidic $-SO_3^-$ groups within its macroreticular matrix. Recently, hydrogenase enzymes, which regulate hydrogen metabolism in nature, have been shown to contain Ni centers in their active sites.[29] This discovery inspired us to investigate model complexes involving mixed donors for application in artificial photosynthesis. For example, an efficient catalyst assembled from a Ni(II) salt and 2-mercaptoethanol was synthesized in one step for photocatalytic hydrogen evolution.[20] A monomeric NiL_2 complex formed between a Ni(II) ion and β-mercaptoethylamine and its derivative trinuclear complex $Ni(NiL_2)_2$ were also evaluated in photocatalytic hydrogen evolution.[30] It is expected that such Ni(II) complexes could be promising catalysts for hydrogen production from water, in which amine ligands act as proton donors and the nickel functions as a hydride donor. Herein, it is shown that the introduction of a trinuclear Ni(II) complex created, during the induction period of the reaction, a new monomeric active species ligated by β-mercaptoethylamine and triethanolamine within the macroreticular space and possessing a $-SO_3^-$ group, which exhibited superior activity, in comparison with a homogeneous Ni precursor, in H_2 production from water under visible light irradiation using xanthene dye as a photosensitizer. We also investigated the effects of functional groups and reaction conditions as well as the recyclability of the catalyst.

RESULTS AND DISCUSSION

Ni complex-exchanged acidic resin was obtained by stirring a suspension of commercially available resins (200CTNa: resin **1**) in H_2O solution containing $Ni(NiL_2)_2Cl_2$ (L = β-mercaptoethylamine) for 3 h at room temperature. Prior to deposition, the resins were crushed by a ball mill (600 rpm for 10 min) to give $Ni_{complex}$/resin **1** (Ni: 0.5 wt %).

As shown in the inset of Figure 1, the UV−vis spectrum of the $Ni(NiL_2)_2Cl_2$ in aqueous solution exhibited a characteristic absorption due to ligand-to-metal charge transfer (262 nm), $^1A_{1g} \rightarrow {}^1B_{2g}$ transition (300 nm), and $^1A_{1g} \rightarrow {}^1A_{2g}$ transition (372 nm) due to a NiS_4 chromophore.[31] The broad and asymmetric bands indicate an overlap of transitions originating from both the terminal NiN_2S_2 and the central NiS_4 moieties. In the spectrum of $Ni_{complex}$/resin **1**, the peak due to ligand-to-metal charge transfer (267 nm) and $^1A_{1g} \rightarrow {}^1B_{2g}$ transition (310 nm) shifted slightly to longer wavelength. In addition, a new peak that was not observed in the original $Ni(NiL_2)_2Cl_2$ or ion-exchange resin **1** was observed at 415 nm. These results

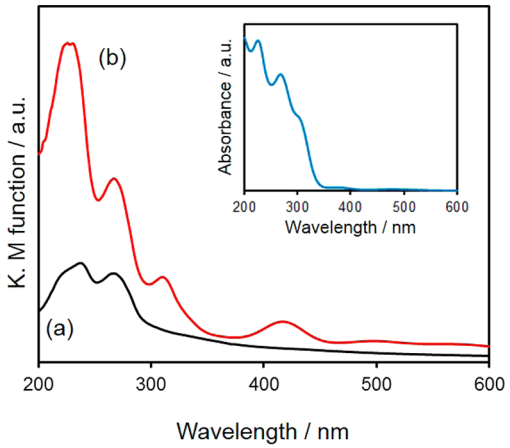

Figure 1. DRUV−vis spectra of (a) acidic resin **1** and (b) $Ni_{complex}$/resin **1**. Inset shows the UV−vis spectrum of $Ni(NiL_2)_2Cl_2$ (L = β-mercaptoethylamine) aqueous solution.

suggested that the local structure around the Ni center was intrinsically different from that of the $Ni(NiL_2)_2Cl_2$ precursor.

X-ray absorption measurements were conducted to elucidate the electronic structure and chemical environment of the exchanged Ni complex. Figure 2A shows normalized X-ray

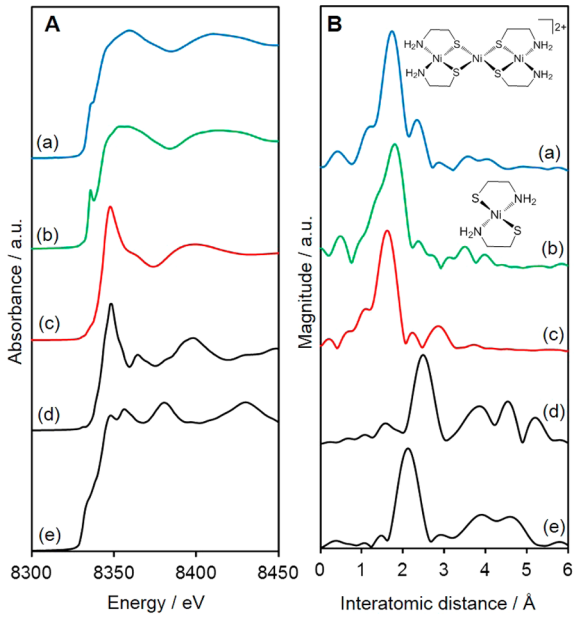

Figure 2. (**A**) Ni K-edge XANES spectra and (**B**) FT-EXAFS spectra of (a) $Ni(NiL_2)_2Cl_2$ (L = β-mercaptoethylamine), (b) NiL_2 (L = β-mercaptoethylamine), (c) $Ni_{complex}$/resin **1**, (d) NiO, and (e) Ni foil.

absorption near-edge structure (XANES) spectra at the Ni K-edge of $Ni_{complex}$/resin **1**, trinuclear $Ni(NiL_2)_2Cl_2$ complex, and monomeric NiL_2 complex, together with NiO and Ni foil as reference samples. The shape and edge position of the XANES spectra of $Ni_{complex}$/resin **1** were similar to those of NiO in an octahedral coordination but differed from those of $Ni(NiL_2)_2Cl_2$ and NiL_2 complexes in square planar coordination and Ni foil. Focusing on the pre-edge region, a small pre-edge peak was observed at around 8331 eV in the case of $Ni_{complex}$/resin **1** and NiO, which was assigned to an electron transition from the Ni 1s orbital to the 3d orbital.[32] In contrast, a larger pre-edge peak was observed at around 8335 eV in the spectra of

dx.doi.org/10.1021/cs501119d | ACS Catal. 2014, 4, 4129−4135

the $Ni(NiL_2)_2Cl_2$ and NiL_2 complexes, which was assigned to the 1s → $4p_z$ transition. In an octahedral coordination environment, 1s → 3d transitions of Ni species are generally forbidden; however, a slight amount of orbital mixing due to lower local symmetry gives some probability for the 1s →3d transition.[33] Therefore, the octahedral Ni species lacked the 1s → $4p_z$ pre-edge peak, while the intensity of the 1s →3d pre-edge peak was smaller than in a square-planar coordination. This reveals that the Ni unit of $Ni_{complex}$/resin **1** are in the 2+ oxidation state in octahedral coordination geometry.

In the Fourier transforms (FT) of the X-ray absorption fine structure (EXAFS) spectra of the $Ni(NiL_2)_2Cl_2$ complex (Figure 2B), a strong peak was observed at around 1.7 Å, which was assigned to Ni−N and Ni−S bonds, in addition to a small second shell at ca. 2.3 Å attributed to neighboring Ni atoms bridged with S atoms. This verifies a trinuclear binding structure for the Ni center in square-planar coordination geometry. In contrast, the peak due to the second shell almost disappeared in the monomeric NiL_2 complex and $Ni_{complex}$/resin **1**. In addition, the main peak of $Ni_{complex}$/resin **1** slightly shifted toward a shorter interatomic distance compared to the $Ni(NiL_2)_2Cl_2$ and NiL_2 complexes, suggesting the substitution of longer Ni−S bonds with shorter Ni−N or Ni−O bonds. In fact, it was confirmed by curve-fitting analysis that the coordination numbers (CN) of the Ni−N(O) shell of $Ni_{complex}$/resin **1** increased in comparison with the other Ni complexes, while the CN of the Ni−S shell decreased after deposition (Table 1). Conclusively, Ni species within the macroreticular resin exist in a monomeric form with octahedral geometry surrounded by a mercaptoethylamine ligand and H_2O. The most reasonable Ni structures are illustrated in Figure 3B. Since the trinuclear $Ni(NiL_2)_2Cl_2$ precursor complex is unstable in acidic solution, we speculate that it easily decomposes to monomeric species such as $[NiL(OH_2)_x]^+$ by the dissociation of Ni−N and/or Ni−S bonds in the presence of acidic resin possessing $-SO_3^-$ group under an aqueous solution. Although there are two types of Ni species in the original trinuclear complex, the formation of $[NiL_2]$ may be ruled out because this electronically neutral complex is only slightly soluble in water and does not have any electrostatic interaction with the $-SO_3^-$ group of ion-exchange resin. In our preliminary experiment, the immobilization of NiL_2 into the resin in an acetone solution was unsuccessful: most of the NiL_2 complex remained intact in solution.

Table 1. Curve-Fitting Analysis of Ni Samples

sample	shell	CN	R/Å	$\Delta\sigma$/Å^2
$Ni(NiL_2)_2Cl_2$	Ni−N	1.4	2.05	0.19
	Ni−S	2.7	2.19	0.065
NiL_2	Ni−N	1.7	2.06	0.02
	Ni−S	2.3	2.20	0.081
$Ni_{complex}$/resin **1**	Ni−N(O)	2.8	2.06	0.044
	Ni−S	1.7	2.18	0.096
$Ni_{complex}$/resin **1**	Ni−N(O)	4.2	2.06	0.024
(isolated after30 min)	Ni−S	1.1	2.19	0.073

Several $Ni_{complex}$/resin catalysts were also prepared from commercially available resins (Amberlite, Rohm and Haas) with different chemical properties. The characteristics of the resins are summarized in Table 2. Resins 200CTNa (resin **1**), 16WET (resin **2**), and 15DRY (resin **3**) were strongly acidic, while FPC3500 (resin **4**) was weakly acidic. Resin 200CTNa and 16WET had a greater water-absorption capacity (swelling property) than 15DRY. ICP analysis determined that the $Ni(NiL_2)_2Cl_2$ complex was easily attached to the above resins at the same level of loading (Ni: 0.5 wt %). All of the resins showed moderate BET-specific surface areas of approximately 45 $m^2\ g^{-1}$. Ni K-edge XAFS analysis showed similar spectra to those of $Ni_{complex}$/resin **1**, suggesting that the Ni species exists in a monomeric form with octahedral geometry within the macroreticular resins (Figure S1). In separate experiments, the deposition of metal complexes on an anion-exchange resin possessing basic groups within its macroreticular matrices was unsuccessful.

In an effort to compare the potential catalytic activity of the $Ni_{complex}$/resins, H_2 production from water was carried out under visible-light irradiation (λ > 420 nm) in H_2O solution containing triethanolamine (TEOA) as a sacrificial reagent and Eosin Y as a photosensitizer. Figure 4 shows the time course of

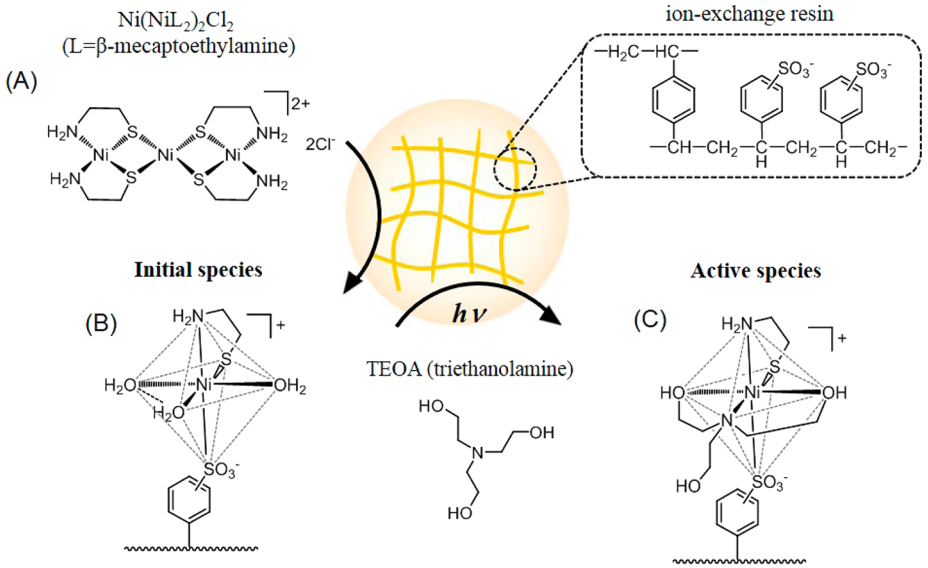

Figure 3. Schematic illustration of transformation of (**A**) $Ni(NiL_2)_2Cl_2$ (L = β-mercaptoethylamine) into (**B**) proposed structure of fresh $Ni_{complex}$/resin **1** and (**C**) *in situ*-generated active species during the photocatalytic reaction.

dx.doi.org/10.1021/cs501119d | ACS Catal. 2014, 4, 4129−4135

Table 2. Textural Properties of Resins

catalyst	resin[a]	functional group	exchange capacity (meq/mL)	property	water absorptioncapacity (%)
$Ni_{complex}$/resin **1**	200CTa	$-SO_3Na$	≥1.8	strongly acidic	46−51
$Ni_{complex}$/resin **2**	16WET	$-SO_3H$	≥1.7	strongly acidic	52−58
$Ni_{complex}$/resin **3**	15Dry	$-SO_3H$	≥2.6	strongly acidic	1−2
$Ni_{complex}$/resin **4**	FPC350	−COOH	≥2.0	weakly acidic	60−70

[a]Styrenic matrix except for resin **4** (acrylic).

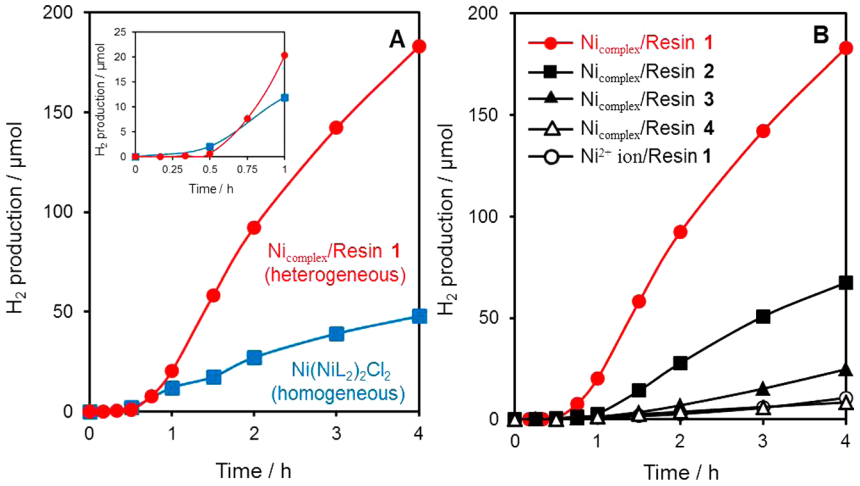

Figure 4. (**A**) Hydrogen production using $Ni_{complex}$/resin **1** and $Ni(NiL_2)_2Cl_2$ (L = β-mercaptoethylamine). The inset shows the induction period in the initial photocatalytic reaction. (**B**) Effect of resin on hydrogen production. Reaction conditions; Ni/resin catalyst (0.1 g, Ni: 0.5 wt %), Eosin Y (0.02 g), 15 vol % TEOA solution (10 mL, pH was adjusted to 8.5 using aqueous HNO_3), Ar atmosphere, Xe lamp (500 W, λ_{ex} > 420 nm) irradiation.

H_2 production using various resin catalysts. Eosin Y was an indispensable component for attaining catalytic activity. No reaction proceeded either under dark conditions in the presence of the $Ni_{complex}$/resins catalyst or without TEOA under light irradiation. Moreover, H_2 production did not occur to any significant extent in the presence of resin **1** without metal complexes under same reaction conditions. It should be noted that the catalytic activity of $Ni_{complex}$/resin **1** (TON = 21) was higher than that of the homogeneous counterparts (TON = 5) by a factor of 4 under such aqueous conditions. The catalytic activity differed significantly according to the resin used, and resin **1**, which had strong acidity as well as a higher water-absorption capacity, was effective among those examined. Since the deposited Ni species existed in an identical structure in each resin catalyst, the macroreticular resin matrix possessing a $-SO_3^-$ group had a significant positive effect, enhancing catalytic activity. The Ni^{2+} ion-exchanged resin catalyst also gave poor results, indicating the necessity of the β-mercaptoethylamine ligand. Under optimizing reaction conditions (amount of TEOA and Ni catalyst), the TOF and TON attained by our $Ni_{complex}$/resin **1** are 19 h^{-1} and 366 (20 h), respectively. It is noteworthy that these values are higher than those recently reported for other heterogeneous Ni catalyst systems, such as $[Ni(TEOA)_2]Cl_2$/g-C_3N_4 (11 h^{-1}, 57 (8 h)),[34] NiS/g-C_3N_4 (3 h^{-1}, 10 (4 h)),[35] and Ni-thiourea-triethylamine/g-C_3N_4 (0.75 h^{-1}, 6 (8 h)).[36]

The pH of the aqueous solution played a significant role in the catalytic activity, because this affected the dielectric constant of the reaction medium. In our catalyst system, the highest activity was attained at pH = 7.5−8.0, and it decreased sharply with decreasing pH, while a gradual decrease was observed with increasing pH (Figure S2). Generally, a decrease in the pH may cause protonation of TEOA to a considerable extent, rendering it a less effective electron donor, while an increase in pH can lead to a decrease in the thermodynamic driving force for H_2 formation. Among the different xanthene dyes evaluated, Erythrosin B was best for the photocatalytic system under discussion. Erythrosin Y also gave a good result, while the use of rose bengal and Eosin Y resulted in slightly lower H_2 production (Figure S3). The difference in the xanthene dyes lies in the halogenation of the xanthene ring; it is known that heavy halogen atoms on the xanthene ring can facilitate the formation of triplet states in xanthene dyes from their excited singlet states through intersystem crossing.[37] Since triplet species have a much longer lifetime in comparison with singlet species, this is advantageous for the transfer of energy and electrons to the Ni catalyst for H_2 production. Another reason may be attributed to the durability of the xanthene dyes. It is reasonable that the xanthene dyes with heavier halogen substituents possess higher stability relative to their lighter-atom counterparts in the test conditions. In our system, Erythrosin B is the most suitable photosensitizer that forms sufficient triplet state species as well as durability.

Interestingly, the time course for H_2 production revealed that the photocatalytic system containing $Ni_{complex}$/resin **1** had an induction period of about 30 min (inset in Figure 4A), in which a concomitant color change of the reaction medium from bright orange to light brown was observed. This phenomenon suggests that the reaction medium transformed the putative catalyst into the real one, due to the significant chemical changes in the Ni species within the resins. To elucidate the structure−activity relationship of this photcatalytic system, the Ni catalyst was isolated and further characterized. In the UV−vis spectrum, the peaks at around 310 and 415 nm in the

dx.doi.org/10.1021/cs501119d | ACS Catal. 2014, 4, 4129−4135

spectrum of fresh $Ni_{complex}$/resin **1** completely disappeared from the spectrum of the isolated compound (Figure S4), indicating a change of local structure around the Ni center during the induction period. As shown in Figure 5A, the Ni K-edge XANES spectrum of the isolated $Ni_{complex}$/resin **1** was similar to that of the fresh product ((a) vs (b)), suggesting that the Ni species retained its monomeric form with octahedral geometry even after the induction period. The FT-EXAFS spectrum of the isolated $Ni_{complex}$/resin **1** also exhibited a strong peak around 1.7 Å attributable to Ni−N(O) and Ni−S bonds, without any shift in comparison with the spectrum of the fresh product (Figure 5B(a) vs (b)). Curve-fitting analysis of the first peak confirmed that the CN of the Ni−N(O) shell increased, accompanied by a decrease in the CN of the Ni−S shell after the induction period (Table 1). Interestingly, an additional new second shell appeared at around 2.5 Å in the isolated $Ni_{complex}$/resin **1**, which was assignable to neighboring carbon atoms. These results verified the involvement of TEOA, a sacrificial reagent (SR) in the photocatalytic H_2 production reaction, as a tridentate binding ligand of the Ni(II) center, because a similar second shell may be observed in the reference $Ni(TEOA)_2Cl_2$ complex (Figure 5B(c)). It can be concluded that the catalytically active species is the *in situ*-generated Ni(II) species surrounded by β-mercaptoethylamine and TEOA ligands within the macroreticular space with a $-SO_3^-$ group during the course of H_2 production. A proposed structure is shown in Figure 3C. The participation of TEOA in the formation of active species is also evidenced by the FT-EXAFS spectra of Ni^{2+} ion/resin **1** after treatment with TEOA and the isolated Ni^{2+} ion/resin **1** after the photocatalytic reaction in the presence of β-mercaptoethylamine, in which an additional new second peak was observed at around 2.5 Å (Figures 5B(d) and (e)).

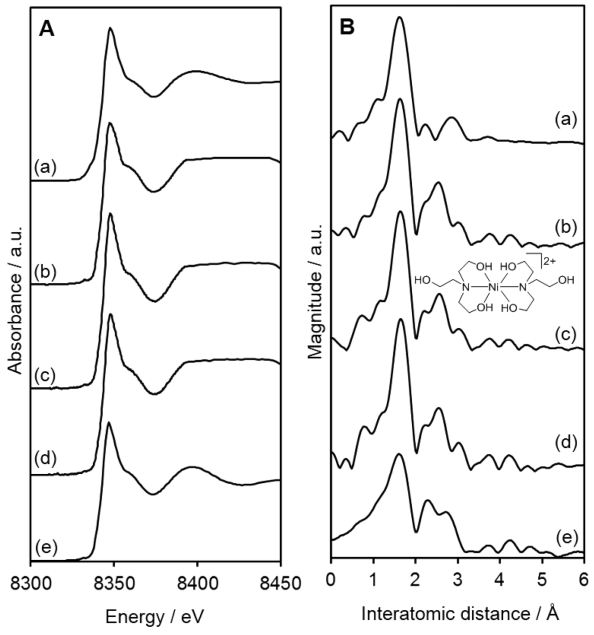

Figure 5. (**A**) Ni K-edge XANES spectra and (**B**) FT-EXAFS spectra of (a) fresh $Ni_{complex}$/resin **1**, (b) isolated $Ni_{complex}$/resin **1** after a 30 min induction period, (c) $Ni(TEOA)_2Cl_2$ complex, (d) Ni^{2+} ion/resin **1** after treatment with TEOA for 30 min, and (e) isolated Ni^{2+} ion/resin **1** after photocatalytic reaction in the presence of β-mercaptoethylamine ligand.

It should be noted that a strongly acidic ion-exchange resin with a $-SO_3H$ group, β-mercaptoethylamine, and TEOA are crucial components for achieving efficient catalytic activity. This contention is supported by the following results: (i) the catalytic activity of heterogeneous $Ni_{complex}$/resin **1** was five times higher than that of the homogeneous counterparts; (ii) the reaction using Ni^{2+} ion-exchanged resin **1** or Ni-$(TEOA)_2^{2+}$/resin **1** without β-mercaptoethylamine resulted in low activity (Figures 4B and 6); (iii) Ni^{2+} ion/resin **1** in the presence of a β-mercaptoethylamine ligand showed a similar reaction rate to $Ni_{complex}$/resin **1**, with a relatively longer induction period (Figure 6); and (iv) the use of triethylamine or EDTA as a sacrificial reagent instead of TEOA gave poor results (data are not shown). In our preliminary experiment, the addition of *p*-toluenesulfonic acid to the reaction mixture of the homogeneous $Ni(NiL_2)_2Cl_2$ complex did not improve the catalytic activity. This result also indicates that not only the $-SO_3H$ group but also the macroreticular structure are important factors in attaining high catalytic activity.

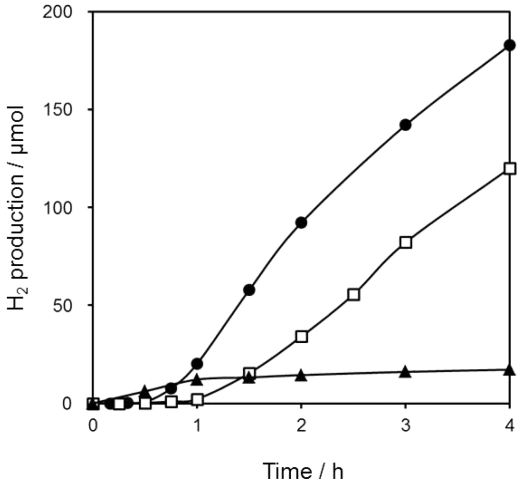

Figure 6. Hydrogen production using $Ni_{complex}$/resin **1** (●), Ni^{2+} ion/resin **1** in the presence of β-mercaptoethylamine ligand (□), and $Ni(TEOA)_2^{2+}$/resin **1**(▲). Reaction conditions; Ni/resin catalyst (0.1 g, Ni: 0.5 wt %), Eosin Y (0.02 g), 15 vol % TEOA solution (10 mL, pH was adjusted to 8.5 using aqueous HNO_3), Ar atmosphere, Xe lamp (500 W, λ_{ex} > 420 nm) irradiation.

There is an argument as to whether H_2 production occurs on metal particles or on the molecular complex.[38,39] As mentioned before, the XAFS spectrum of the recovered $Ni_{complex}$/resin **1** retained its monomeric form even after the photocatalytic reaction without detection of a Ni−Ni bond (Figure 5B). Moreover, the $Ni_{complex}$/resin can be recycled at least three times (Figure S5), suggesting that this reaction proceeds on the molecular species exchanged within the macroreticular space of the resin. This is a strong evidence showing that the molecular species, rather than the colloidal form, is responsible for catalysis. Unfortunately, the catalytic activity is apparently decreased in the third cycle which is around 70% of that from fresh catalyst. The dropping of activity may be caused by the slight loss of catalyst particles during centrifugation in the recycling experiment. Another explanation is the decomposition of ion-exchange resin during photoirradiation, which may cause the deterioration of surface functional groups.

As described earlier, the classical molecular-based photocatalytic H_2 production system consists of many components,

dx.doi.org/10.1021/cs501119d | *ACS Catal.* 2014, 4, 4129−4135

including a PS ($Ru(bpy)_3^{2+}$), an ER (methyl viologen), a WRC (colloidal Pt), and an SR. The electron relay step is generally crucial to the success of the photocatalytic system; an efficient ER oxidatively quenches the excited PS, thereby allowing charge separation, although at the expense of simplicity. On the other hand, the use of heavy halogen-substituted xanthene dyes enables direct injection of electrons to the Ni catalyst without an ER, owing to their high intersystem crossing yields, which are favorable for the formation of the long-lived $3\pi\pi^*$ triplet state.[30] In the photoluminescence spectra of EosinY, the emission peak located at 530 nm gradually decreased with increasing the amount of Ni complex. Such strong emission quenching is caused by the electron transfer from the dye molecules to the Ni complex (Figure S6). A possible reaction pathway is illustrated in Scheme S1. First, the Ni species is protonated, receiving a proton from water at the amine moiety, which accepts an electron from the excited triplet state of the Eosin Y photosensitizer, accompanied by reduction of Ni(II) to Ni(I). In alignment with this step, the proton is transferred from the N atom to the Ni center to form a hydride intermediate. Subsequent additional electron transfer and protonation of amino groups afford the key $Ni-H^-/N-H^+$ intermediates in close proximity, which finally form a H−H bond as the expected product. Separately, the oxidized PS is reduced by the sacrificial TEOA electron donor. In simple terms, this reaction is facilitated by direct electron transfer from the photosensitizer Eosin Y to the proton reduction catalyst (the Ni complex) without an electron mediator. Based on theoretical and experimental studies, it has been suggested that basic N atoms near the metal center can function as an intramolecular proton transfer relay for achieving efficient H_2 production and that the formation of a H−H bond from the $Ni-H^-/N-H^+$ intermediate is the rate-determining step in the overall catalytic cycle.[40−42] This assumption also supports the importance of the β-mercaptoethylamine ligand; reactions using Ni^{2+} ion-exchanged resin **1** or $Ni(TEOA)_2^{2+}$/resin **1** in the absence of β-mercaptoethylamine gave poor results. Preliminary kinetic studies found that the reaction rate showed a first-order dependence on the loading amount of Ni used and a 0.5-order relationship with the amount of Eosin Y (Figures S7 and S8), which supports the above-described mechanism involving two consecutive reductions of Ni species by Eosin Y to generate one equivalent of H_2 molecules. The macroreticular environment of the resin may not only facilitate efficient H^+ transfer through $-SO_3^-$ groups but also provide for close proximity between the Ni complex and the PS, which assists the cooperative action of adjacent molecules, thus ultimately enhancing the H_2 evolution activity.

CONCLUSION

Treatment of the trinuclear complex $Ni(NiL_2)_2Cl_2$ (L = β-mercaptoethylamine) with an ion exchange acidic resin created a noble-metal-free Ni-based catalyst for H_2 production from water. Ni K-edge X-ray absorption fine structure (XAFS) measurement suggested that a monomeric Ni(II) complex coordinated to a β-mercaptoethylamine ligand was accommodated in the macroreticular space with a $-SO_3^-$ group ($Ni_{complex}$/resin), which was transformed into an active Ni(II) species in the presence of triethanolamine (TEOA) during the initial induction period of the photocatalytic reaction. A strongly acidic ion-exchange resin with a $-SO_3^-$ group, β-mercaptoethylamine, and TEOA were indispensable factors in achieving high catalytic activity. The $Ni_{complex}$/resin behaved as a heterogeneous catalyst enabling efficient H_2 production when xanthene dye was employed as a visible-light-responsive photosensitizer, with an activity five times higher than that of its homogeneous counterpart. Further studies are currently ongoing to develop noble-metal-free catalysts with enhanced activity and durability.

EXPERIMENTAL SECTION

Materials. 2-Mercaptoethylamine hydrochloride, nickel chloride hexahydrate, Eosin Y (EY), and triethanolamine (TEOA) were purchased from Aldrich. These reagents were analytical grade and were used without further purification. All resins were Amberlite, supplied by Rohm and Haas.

Synthesis of $[Ni(Ni(NH_2CH_2CH_2S)_2)_2]Cl_2$ $[Ni(NiL_2)_2Cl_2]$.[30] 26.4 mmol of 2-mercaptoethylamine hydrochloride was dissolved in 25 mL of ethanol solution. A second solution was prepared by dissolving 52.8 mmol of sodium hydroxide in 100 mL of water/ethanol = 2:3 solution, which was added to the first solution, followed by removal of sodium chloride formed during the neutralization by filtration. This ligand solution was then added dropwise to a 30 mL aqueous solution containing 20 mmol of $NiCl_2{\cdot}6H_2O$ at 60 °C under magnetic stirring. The solution turned red in color, and dark green crystals were precipitated. After complete addition of the ligand, the solution was allowed to stand in an ice bath for 2 h.

Synthesis of Catalyst. Several Ni catalysts were prepared from commercially available resins (Amberlite, Rohm and Haas) with different chemical properties. Prior to deposition, resins were crushed by a ball mill (600 rpm for 10 min). An aqueous solution of $Ni(NiL_2)_2Cl_2$ (30 mL) was mixed with the resin (1.0 g), and the resultant mixture was stirred for 3 h at room temperature. The mixture was filtered, and the resulting solid was washed repeatedly with distilled water and dried overnight, giving $Ni_{complex}$/resin (Ni: 0.5 wt %). Other samples with different resins were also prepared by the same method. Metal loadings were determined by inductively coupled plasma (ICP) analysis.

Characterization. BET surface area measurements were performed using a BEL-SORP max (Bel Japan, Inc.) instrument at 77 K. The sample was degassed under vacuum at 353 K for 24 h prior to data collection. UV−vis diffuse reflectance spectra of powdered samples were collected using a Shimadzu UV-2450 spectrophotometer. The reference was $BaSO_4$, and the absorption spectra were obtained using the Kubelka−Munk function. Inductively coupled plasma optical emission spectrometry (ICP-OES) measurements were performed using a Nippon Jarrell-Ash ICAP-575 Mark II instrument. Ni K-edge XAFS spectra were recorded using a fluorescence-yield collection technique at the beamline 01B1 station with an attached Si (111) monochromator at SPring-8, JASRI, Harima, Japan (prop. no. 2013B1041 and 2014A1045). The EXAFS data were normalized by fitting the background absorption coefficient, around the energy region higher than that of the edge of about 35−50 eV, with smooth absorption of an isolated atom. The EXAFS data were examined using the Rigaku EXAFS analysis program. Fourier transformation (FT) of k^3-weighted normalized EXAFS data was performed over the 3.5 Å < k/Å^{-1} < 11 Å range to obtain the radial structure function.

Photocatalytic H_2 Production. The powdered Ni/resin catalyst (0.1 g), Eosin Y (0.02 g), and 15 vol % triethanolamine (TEOA) solution (10 mL) were introduced into a Pyrex reaction vessel (30 mL) which was then sealed with a rubber septum. The pH value of the TEOA solution was first adjusted

dx.doi.org/10.1021/cs501119d | ACS Catal. 2014, 4, 4129−4135

to 8.5 using concentrated aqueous HNO_3 solution. The resulting mixture was bubbled with Ar for 15 min in dark conditions. Subsequently, the sample was irradiated from the side using a Xe lamp (500 W; SAN-EI Electric Co., Ltd. XEF-501S) through a glass filter ($\lambda > 420$ nm) with magnetic stirring at ambient pressure and temperature. The reaction progress was monitored using a Shimadzu GC-14B instrument equipped with MS5A columns.

■ ASSOCIATED CONTENT

Supporting Information

XAFS spectra of Ni/resin catalysts, effect of pH, loading amount of $Ni_{complex}$/resin, and loading amount of Eosin Y in hydrogen production, DRUV−vis spectrum of the isolated catalyst, recycling experiments, and photoluminescence spectra. This material is available free of charge via the Internet at http://pubs.acs.org.

■ AUTHOR INFORMATION

Corresponding Authors

*Phone: 81-6-6879-7460. Fax: 81-6-6105-5029. E-mail: mori@mat.eng.osaka-u.ac.jp.

*Phone/Fax: 81-6-6879-7457. E-mail: yamashita@mat.eng.osaka-u.ac.jp.

Notes

The authors declare no competing financial interest.

■ ACKNOWLEDGMENTS

The present work was supported by the Grant-in-Aid for Scientific Research from the Ministry of Education, Culture, Sports, Science and Technology of Japan (252892890) and JSPS Asian CORE Program. A part of this work was also performed under a management of 'Elements Strategy Initiative for Catalysts & Batteries (ESICB)' supported by MEXT.

■ REFERENCES

(1) Lewis, N. S.; Nocera, D. G. *Proc. Natl. Acad. Sci. U. S. A.* **2006**, *103*, 15729−15735.

(2) Eisenberg, R. *Science* **2009**, *324*, 44−45.

(3) Graetzel, M. *Acc. Chem. Res.* **1981**, *14*, 376−384.

(4) Esswein, A. J.; Nocera, D. G. *Chem. Rev.* **2007**, *107*, 4022−4047.

(5) Bard, A. J.; Fox, M. A. *Acc. Chem. Res.* **1995**, *28*, 141−145.

(6) Fujishima, A.; Honda, K. *Nature* **1972**, *238*, 37−38.

(7) Gratzel, M. *Nature* **2001**, *414*, 338−344.

(8) Arakawa, H.; Sayama, K. *Catal. Surv. Jpn.* **2000**, *4*, 75−80.

(9) Maeda, K.; Domen, K. *J. Phys. Chem. C* **2007**, *111*, 7851−7861.

(10) Kudo, A.; Miseki, Y. *Chem. Soc. Rev.* **2009**, *38*, 253−278.

(11) Tinker, L. L.; McDaniel, N. D.; Bernhard, S. *J. Mater. Chem.* **2009**, *19*, 3328−3337.

(12) Wang, M.; Na, Y.; Gorlov, M.; Sun, L. *Dalton Trans.* **2009**, 6458−6467.

(13) Tran, P. D.; Artero, V.; Fontecave, M. *Energy Environ. Sci.* **2010**, *3*, 727−747.

(14) Ozawa, H.; Sakai, K. *Chem. Commun.* **2011**, *47*, 2227−2242.

(15) Mori, K.; Kawashima, M.; Che, M.; Yamashita, H. *Angew. Chem., Int. Ed.* **2010**, *49*, 8598−8601.

(16) Kirch, M.; Lehn, J.-M.; Sauvage, J.-P. *Helv. Chim. Acta* **1979**, *62*, 1345−1384.

(17) Streich, D.; Astuti, Y.; Orlandi, M.; Schwartz, L.; Lomoth, R.; Hammarström, L.; Ott, S. *Chem.—Eur. J.* **2010**, *16*, 60−63.

(18) Lazarides, T.; McCormick, T.; Du, P.; Luo, G.; Lindley, B.; Eisenberg, R. *J. Am. Chem. Soc.* **2009**, *131*, 9192−9194.

(19) McNamara, W. R.; Han, Z.; Alperin, P. J.; Brennessel, W. W.; Holland, P. L.; Eisenberg, R. *J. Am. Chem. Soc.* **2011**, *133*, 15368−15371.

(20) Zhang, W.; Hong, J.; Zheng, J.; Huang, Z.; Zhou, J.; Xu, R. *J. Am. Chem. Soc.* **2011**, *133*, 20680−20683.

(21) Han, Z.; Shen, L.; Brennessel, W. W.; Holland, P. L.; Eisenberg, R. *J. Am. Chem. Soc.* **2013**, *135*, 14659−14669.

(22) Leadbeater, N. E.; Marco, M. *Chem. Rev.* **2002**, *102*, 3217−3274.

(23) Roth, W. J.; Nachtigall, P.; Morris, R. E.; Čejka, J. *Chem. Rev.* **2014**, *114*, 4807−4837.

(24) McNamara, C. A.; Dixon, M. J.; Bradley, M. *Chem. Rev.* **2002**, *102*, 3275−3300.

(25) Mori, K.; Kubota, Y.; Yamashita, H. *Chem.—Asian J.* **2013**, *8*, 3207−3213.

(26) Mori, K.; Dojo, M.; Yamashita, H. *ACS Catal.* **2013**, *3*, 1114−1119.

(27) Mori, K.; Hanafusa, A.; Che, M.; Yamashita, H. *J. Phys. Chem. Lett.* **2010**, *1*, 1675−1678.

(28) Zhang, F.; Yang, X.; Zhu, F.; Huang, J.; He, W.; Wang, W.; Li, H. *Chem. Sci.* **2012**, *3*, 476−484.

(29) Fontecilla-Camps, J. C.; Volbeda, A.; Cavazza, C.; Nicolet, Y. *Chem. Rev.* **2007**, *107*, 4273−4303.

(30) Han, J.; Zhang, W.; Zhou, T.; Wang, X.; Xu, R. *RSC Adv.* **2012**, *2*, 8293−8296.

(31) Turner, M. A.; Driessen, W. L.; Reedijk, J. *Inorg. Chem.* **1990**, *29*, 3331−3335.

(32) Colpas, G. J.; Maroney, M. J.; Bagyinka, C.; Kumar, M.; Willis, W. S.; Suib, S. L.; Mascharak, P. K.; Baidya, N. *Inorg. Chem.* **1991**, *30*, 920−928.

(33) Asakura, H.; Shishido, T.; Tanaka, T. *J. Phys. Chem. A* **2012**, *116*, 4029−4034.

(34) Dong, J.; Wang, M.; Li, X.; Chen, L.; He, Y.; Sun, L. *ChemSusChem* **2012**, *5*, 2133−2138.

(35) Hong, J.; Wang, Y.; Wang, Y.; Zhang, W.; Xu, R. *ChemSusChem* **2013**, *6*, 2263−2268.

(36) Wang, D.; Zhang, Y.; Chen, W. *Chem. Commun.* **2014**, *50*, 1754−1756.

(37) Shimidzu, T.; Iyoda, T.; Koide, Y. *J. Am. Chem. Soc.* **1985**, *107*, 35−41.

(38) Lei, P.; Hedlund, M.; Lomoth, R.; Rensmo, H.; Johansson, O.; Hammarström, L. *J. Am. Chem. Soc.* **2007**, *130*, 26−27.

(39) Wang, C.; Cao, S.; Fu, W.-F. *Chem. Commun.* **2013**, *49*, 11251−11253.

(40) Kilgore, U. J.; Stewart, M. P.; Helm, M. L.; Dougherty, W. G.; Kassel, W. S.; DuBois, M. R.; DuBois, D. L.; Bullock, R. M. *Inorg. Chem.* **2011**, *50*, 10908−10918.

(41) Pandey, A. S.; Harris, T. V.; Giles, L. J.; Peters, J. W.; Szilagyi, R. K. *J. Am. Chem. Soc.* **2008**, *130*, 4533−4540.

(42) Rakowski DuBois, M.; DuBois, D. L. *Chem. Soc. Rev.* **2009**, *38*, 62−72.